Determining the Accelerating Expansion of the Universe by Observing Type Ia Supernovae

Duo Tao

May 12, 2018

Abstract

We study the accelerating expansion of the Universe by observing Type Ia supernovae, which happens when a white dwarf becomes unstable after its mass exceeds the Chandrasekhar limit. We start by showing theoretically how to measure the acceleration of the Universe expansion. We present the mechanism of Type Ia supernovae and explain why we choose to use them in measuring the acceleration. We also introduce the charge-coupled devices, which help us to detect enough high-redshift Type Ia supernovae. Finally, we present the experimental results and show that the Universe expansion is accelerating.

Contents

1 Introduction

At the beginning of the last century, physicists and astronomers started making efforts to understand the Universe by observing a class of celestial events [1]. In 1912, Henrietta Swan Leavitt, an American astronomer, studied thousands of variable stars, stars with periodic change of brightness, and found that higher brightness was correlated with longer periods. Since we know the distances to some nearby variable stars[1], we can calculate their luminosities. Leavitt discovered a relation between the period and the luminosity in these nearby stars. She extrapolated this relation to find out the luminosities of the distant stars. Knowing the luminosity and the brightness of a distant star, she was able to calculate the distance to the variable stars.

Also in 1912, Vesto Slipher was working on the Andromeda Nebula and observed redshifts and calculated the velocity of the distant stars [2]. Later in the 1920s, with the completion of the Mount Wilson telescope, we found that all galaxies were moving away from us. Another American astronomer, Edwin Hubble combined Leavitt's data to calculate the distances to the variable stars with Vesto Slipher's method of measuring the receding velocities. He found a relation between the receding velocity and the distance. We named this relation after him as Hubble's law [1]. Hubble's law is evidence that the Universe is expanding.

With the introduction of general relativity by Albert Einstein, different cosmological models using general relativity were established to explain the expansion of the Universe. One of the models developed was the Robertson-Walker metric, which assumed the Universe was homogeneous and isotropic, inserting a time-dependent expansion term into the metric equation to indicate the change of scale of the Universe with time. General relativity requires that the Universe either shrinks or expands [1]. Thus, the need to measure the acceleration or deceleration of the Universe appeared. As is determined by the Robertson-Walker metric, measuring the acceleration requires observation of more distant objects. It turns out that the variable stars are too faint for this. Therefore, we were in need of a new class of objects with standard luminosities that were bright enough to measure at great distances.

In 1938, Baade proposed that we could use Type Ia supernovae for this purpose [3]. In that paper, he studied the spectra and the brightness of some supernovae detected at that time. These studies suggest that these supernovae could serve well to measure the deceleration parameter at higher redshift. However, at that time, we did not have the technology to collect enough data with enough precision. With the technology developments in the late 1990s, scientists were able to pick up the work and successfully measured the cosmological deceleration parameters, and this led to the Nobel Prize in 2011 [1, 4, 5].

In this paper, we follow the steps of the Nobel Laureates to understand the acceleration of the Universe

[1] We could find out the distances of nearby stars using parallax measurements.

expansion. In section 2, we are going to theoretically explain what the acceleration of the expansion is and how we relate it to the supernovae. In section 3, we present the experiments, use the theories to understand the results and eventually reach the conclusion that the expansion is accelerating.

2 Cosmological Mechanism

In this section, we will explain how we can measure the expansion acceleration with Type Ia supernovae. We will start by introducing two quantities that we can directly calculate from observations, the luminosity distance and the redshift. We can calculate them from the brightness and the spectra of the supernovae, respectively. Then we use general relativity to derive a relation between them. The relation involves the energy components of the Universe, which can directly determine the expansion acceleration. Therefore, we can measure the acceleration of the expansion by deducing the values of the energy components once we have enough observations.

2.1 Redshift

We start by introducing redshift. According to Doppler's effect, we know that when the source of a wave and a receiver recede from each other, the wavelength received will be longer than the wavelength sent. This is Doppler's effect. If we send a wave with wavelength λ_1, in the receiver's frame, the wavelength received λ_o will be

$$\frac{1}{\lambda_o} = \frac{c}{c + v_s}\frac{1}{\lambda_1} \tag{1}$$

where c is the speed of light, and v_s is the speed of the source. The speed v_s is positive when the source is moving away from the receiver and negative if moving towards the receiver. When we set $c = 1$ in Eq. 1, we have

$$z \equiv \frac{\Delta\lambda}{\lambda_1} = \frac{\lambda_o - \lambda_1}{\lambda_1} = v_s \tag{2}$$

Eq. 2 defines redshift in terms of the wavelength difference $\Delta\lambda$. When the source moves away from the receiver, the speed v_s is positive and the wavelength $\Delta\lambda$ is also positive, which means the wavelength increases. Thus, a receding source will give a redshifted light.

In other words, we can use redshift to calculate the receding speed of the source by Eq. 2. This effect was first studied and used to calculate the receding speed by Vesto Slipher in 1913 [2]. Because of Hubble's law [6], which claims that the receding speed of a galaxy is proportional to the distance from the earth, we

commonly use redshift to indicate distance.

2.2 Luminosity distance

Now we introduce luminosity distance. When we observe a distant galaxy with luminosity L, we can measure its brightness B. The inverse square law gives their relation as

$$B = \frac{L}{4\pi d_L^2} \tag{3}$$

where d_L is the luminosity distance. Usually, in a flat universe, the luminosity distance d_L is the same as the spatial distance. However, when we take into account the Universe expansion, the situation becomes more complicated. The scale of the Universe changes with time and thus when the light travels to Earth, the Universe expands and the spatial interval at the time of emission will be smaller than the interval at its arrival. Also, we should consider redshift since as the wavelength increases the energy of the photons decreases. Besides, if spatial interval increases between photons, the time gap between each photon also increases.

Therefore, the relation between the luminosity and the brightness involves more terms than the spatial distance. We pack all the variations into a new quantity called luminosity distance. Rewriting the inverse square law, we define luminosity distance as [7]

$$d_L \equiv \sqrt{L/(4\pi B)}. \tag{4}$$

Note that the brightness B can be directly observed. If the observation object is a standard candle, an object that we know its luminosity L, we can calculate the luminosity distance d_L. Type Ia supernovae are standard candles, having almost uniform luminosities. Therefore, we can calculate their luminosity distances.

2.3 Luminosity distance - redshift relation

Now that we have introduced the redshift and the luminosity distance, we will derive a relation between them. We start by stating and explaining a fundamental assumption, the cosmological principle, which enables us to treat the Universe in a simpler way. From the cosmological principle, we build the Robertson-Walker metric, where we can start our journey of general relativity. The Einstein equation requires the metric to follow certain relations between the expansion of the Universe and the energy density in the Universe. This

leads to the Friedmann equations. After introducing the redshift, the luminosity distance and the energy components, the Friedmann equations become the luminosity distance-redshift relation. We will present this relation in two forms: the series form and the integral form.

We present the series form in order to see on what order of the redshift we can measure the acceleration. We treat the relation as an unknown function and use Taylor expansion on it. We find that the first order term, as is expected in Hubble's law, has only Hubble's constant. In the second order term, however, we see the acceleration effects. Therefore, in order to measure the acceleration, we need to have precise measurements of supernovae with higher redshift to see the effect of the second order term.

After the series form, we derive the integral form of the relation. The integral form of the relation is what we use directly in the experiment. The Friedmann equations introduce the energy components into the picture. The scale of the Universe is related to both the redshift and the luminosity distance. Therefore, we can substitute the redshift and the luminosity distance for the scale of the Universe, thereby arriving at a closed form of the luminosity distance-redshift relation.

2.3.1 Cosmological principle

Based on the observations of Hubble and other astronomers in that era, astronomers started to make some fundamental assumptions about the Universe in order to build and test models from experimental observations. Among them, one of the most profound is the cosmological principle [8], illustrated in Fig. 1. The principle was first stated by Issac Newton and then put into use when astronomers started to gather evidence and build models about it at the start of the 20th century. The cosmological principle states that the Universe is homogeneous and that the Universe is isotropic. Both statements are symmetric assumptions which simplify the Universe on a cosmological scale [9].

1. *Homogeneous.* Homogeneity means that the Universe is the same everywhere. We are in no special position in the Universe. This assumption enables us to assume some uniform parameters such as energy density across the Universe.

2. *Isotropic.* Isotropism means that from the perspective of the Earth, the Universe is the same in all directions. Considering the fact that there is no special position in the Universe, this leads to the fact that the Universe is boundless since, assuming it is bounded, we can extend to one direction forever by moving the observer to the boundary.

The cosmological principle is an assumption of symmetry. There is neither a place nor a direction that is

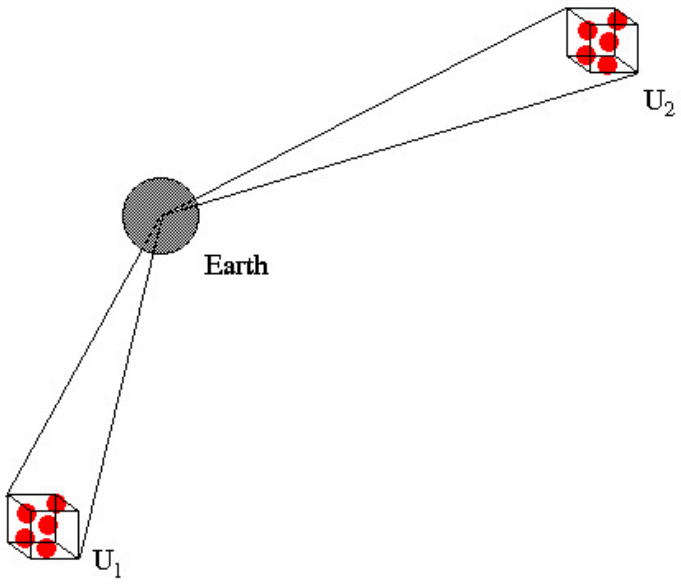

Figure 1: An illustration of the cosmological principle [10]. The picture shows both the isotropic assumption and the homogeneous assumption. Samples U_1 and U_2 are in different directions from the Earth. They are also at different positions in the Universe. However, by the cosmological principle, the contents contained in U_1 and U_2 are the same on a large scale.

different from others. It views the Universe on a large scale and ignores local characteristics. It is also a more fundamental way to understand the law in the Universe. Because the same law is applied, matter and energy do not favor any position in the Universe over another.

2.3.2 Robertson-Walker metric

Based on the cosmological principle, we can build a powerful model with general relativity that serves as the theoretical foundation of the accelerating expansion of the Universe [11]. We construct the metric from a flat spacetime without any expansion of the Universe[2]

$$ds^2 = -dt^2 + dr^2 + r^2 d\theta^2 + r^2 \sin^2\theta d\phi^2. \tag{5}$$

The flat spacetime is coherent with the cosmological principle. It is the only way for the spacetime to be isotropic and homogeneous. When we add the expansion into the metric, it has to be an overall factor over

[2]The flat assumption is valid according to the cosmic microwave background (CMB) studies [12] [7].

all of the spatial coordinates. Otherwise, the flatness of the spacetime will break down over time, violating the cosmological principle. Then, we have the Robertson-Walker metric as

$$ds^2 = -dt^2 + a(t)[dr^2 + r^2 d\theta^2 + r^2 \sin^2\theta d\phi^2]. \tag{6}$$

We can understand the time-dependent factor $a(t)$ as the spatial scale of the Universe. Because the $a(t)$ term accounts for all the expansion, other parameters are independent of time. Hence, in this coordinate system, a galaxy has fixed coordinates as the Universe expands.

2.3.3 Friedmann equations

The Friedmann equations are the Einstein equation for the Robertson-Walker metric. They relate the scale of the universe with the energy density ρ, which, as we will see, is necessary for the acceleration of the expansion. We will use the Einstein equation on the Robertson-Walker metric defined in Eq. 6 to derive a relation between the energy in the Universe and the scale $a(t)$ [7].

We start from the Einstein equation in the form of Ricci tensor R_{uv} and energy momentum tensor T_{uv}:

$$R_{uv} = -8\pi G(T_{uv} - \frac{1}{2} g_{uv} T) \tag{7}$$

where g_{uv} is the metric tensor, a tensor that only has the diagonal terms as given by Eq. 6. The scalar T is defined as $T \equiv g^{uv} T_{uv}$. The energy momentum tensor T_{uv} describes the energy and matter distribution in the Universe. The Ricci tensor R_{uv} describes the curvature of the Universe and depends on the metric tensor g_{uv}. The Einstein equation governs the interaction between matter and spacetime[3]. We plug in the Robertson-Walker metric in Eq. 6 to find the components of the Ricci tensor. We can write the Ricci tensor in terms of $a(t)$,

$$R_{ij} = -(2\dot{a}^2 + a\ddot{a}) g_{ij} \tag{8a}$$

$$R_{tt} = 3\frac{\ddot{a}}{a}. \tag{8b}$$

In Eq. 8, labels i and j are spatial parameters. All other components, R_{0i} or R_{i0}, vanish.

The galaxies in the Universe are similar to air molecules floating around, randomly moving in space. By this property, we assume the Universe to be a perfect fluid of galaxies. We know the T_{tt} term is the energy

[3]It would be too much digression to give a full discussion on everything involved in the Einstein equation. For more details, please refer to *A General Relativity Notebook*, by Thomas A. Moore [11].

density $-\rho$. Assuming the perfect fluid, we know the pressure in all directions to be the same, and there is no other way of transferring momentum than the normal pressure. Hence, all the off diagonal terms vanish. The energy momentum tensor T_{uv} becomes [11]

$$\begin{aligned} T_{tt} &= -\rho, \\ T_{ii} &= p, \end{aligned} \tag{9}$$

where p is the pressure of the perfect fluid. Plugging the Ricci tensor in Eq. 8 and the energy momentum tensor in Eq. 9 into the Einstein equation in Eq. 7, we get the Friedmann equations

$$-(2\dot{a}^2 + a\ddot{a}) = 4\pi G(\rho - p)a^2 \tag{10a}$$

$$\frac{3\ddot{a}}{a} = -4\pi G(\rho + 3p). \tag{10b}$$

From Eq. 10, we arrive at another form as

$$\dot{a}^2 = \frac{8\pi G\rho a^2}{3}. \tag{11}$$

The Friedmann equation relates the energy density ρ of the Universe with its expansion $\dot{a}$[4].

2.3.4 Series form of the luminosity distance-redshift relation

Next, we will express the luminosity distance with the redshift z as a power series [7]. We will find that the acceleration shows up on the second order term in the series. Therefore, to measure the effect of the acceleration, we must make observations at higher redshift.

Based on a radial photon motion with $\Delta s^2 = 0$ and the Robertson-Walker metric expressed in Eq. 6, we get

$$dt^2 = a^2(t)dr^2. \tag{12}$$

If we integrate from the emission time t_e to the observation time t_0, we get

$$\int_{t_e}^{t_0} \frac{dt}{a(t)} = d_p(t_0) \tag{13}$$

where $d_p(t_0)$ is the current light path length. It is equal to the radial coordinate r if we normalize the current

[4]All of Eq. 10 and Eq. 11 can be called Friedmann equations since they all relate the expansion term $a(t)$ to the energy and matter. In this paper, we will specify when we use them.

scale factor a_0.

We use Taylor expansion on $a(t)$ and get

$$a(t) = a(t_0) + \frac{da}{dt}(t - t_0) + \frac{1}{2}\frac{d^2a}{dt^2}(t - t_0)^2. \tag{14}$$

If we normalize $a(t_0) = 1$ and keep the first two terms (the reason of which shall be clear soon), the expansion becomes

$$a(t) = 1 + \dot{a}(t - t_0) + \frac{1}{2}\ddot{a}(t - t_0)^2. \tag{15}$$

Also, if we imagine a galaxy at the edge of our Universe, we have a variation of the Hubble's law [6] based on $a(t)$,

$$H_0 = \frac{\dot{a}}{a}. \tag{16}$$

We define a dimensionless quantity, deceleration parameter[5] q_0, as

$$q_0 \equiv -\frac{a\ddot{a}}{\dot{a}^2}. \tag{17}$$

The deceleration parameter q_0 is positive if the expansion is decelerating and negative if accelerating. Thus, based on the deceleration parameter in Eq. 17 and the Hubble constant in Eq. 16, we can rewrite the Taylor expansion in Eq. 15 as

$$a(t) = 1 + H_0(t - t_0) + \frac{1}{2}\ddot{a}(t - t_0)^2. \tag{18}$$

We find the Taylor expansion of $1/a(t)$ to be

$$\frac{1}{a(t)} = 1 + \dot{a}(t - t_0) = 1 - H_0(t - t_0). \tag{19}$$

Integrating the expansion in Eq. 13, we find an expansion of the light path length d_p in terms of the time elapse $t_0 - t_e$ as

$$d_p(t_0) = (t_0 - t_e) + \frac{H_0}{2}(t_0 - t_e)^2. \tag{20}$$

Here we shall reinvestigate the concept of luminosity distance defined in Eq. 4 in the context of an expanding Universe [7]. When a photon is emitted and received at the Earth, there are three effects contributing to the attenuation of the light energy: the inverse square law, the redshift, and the increase of distance between

[5]By convention, we call q_0 deceleration parameter because scientists believed the Universe expansion was decelerating due to the gravitational effect.

each photon.

1. Inverse square law gives a factor of $1/d_p^2$.
2. The redshift gives a factor of $a(t_e)$.
3. The increase of interval gives another factor of $a(t_e)$. The spacetime interval gap increases so the time required for the next photon to land increases. Thus, the energy delivered per second decreases.

Based on the three effects, the inverse square law becomes

$$B = \frac{L}{4\pi d_p^2} a^2(t_e). \tag{21}$$

Now we shall look into a relation between the expansion factor $a(t)$ and the redshift z. We know the redshift z is defined in Eq. 2. As the Universe expands, we know $\lambda_o/\lambda_1 = a(t_e)$. Thus, we have this relation

$$\frac{1}{a(t_e)} = z + 1. \tag{22}$$

From the definition of luminosity distance in Eq. 4, Eq. 21 and Eq. 22, we notice that now the luminosity distance can be written as

$$d_L = d_p(1 + z). \tag{23}$$

Now that we have the relation between $a(t)$ and the redshift z in Eq. 22, we can rewrite the expansion of $a(t)$ in Eq. 18 as

$$z = H_0(t - t_0) + \frac{1}{2}(q_0 + 2)H_0^2(t_0 - t_1)^2 \tag{24}$$

Inverting this series by calculating the expansion of f^{-1}, we get

$$H_0(t_0 - t_1) = z - \frac{1}{2}(q_0 + 2)z^2. \tag{25}$$

We plug the above equation into the expansion of d_p in Eq. 20 to get d_p in terms of the redshift z. Using Eq. 23 to get the luminosity distance from d_p, we find the series form of the luminosity distance-redshift relation as [7]

$$d_L = \frac{1}{H_0}\big(z + \frac{1}{2}(1 - q_0)z^2\big). \tag{26}$$

We notice that the deceleration parameter q_0 appears in the second order term. Therefore, we must measure d_L at high redshift to extract the effect of the z^2 term.

2.3.5 Integral form of the luminosity distance-redshift relation

In this section, we use the Friedmann equations in Eq. 11 to derive an integral form of the luminosity distance-redshift relation [7]. The integral form of the relation is the essential theoretical part of this study since the experiment uses this relation to deduce the energy components, which then determines the acceleration of the Universe expansion.

Before we start, we define the critical density ρ_c from the Friedmann equation as

$$\rho_c \equiv \frac{3H_0^2}{8\pi G}. \tag{27}$$

The critical density is the energy density required for a flat Universe. There should have been a curvature term on the left-hand side as a constant but since we assume a flat Universe [7], it goes away.

With the critical density defined as a constant, we can normalize the energy density by taking the ratio to the critical density as

$$\Omega \equiv \frac{\rho}{\rho_c}. \tag{28}$$

Now we can get an expression of the energy density ρ in terms of the energy components. We assume there are two components in the Universe, energy of regular matter ρ_R and vacuum energy ρ_Λ. General relativity requires that ρ_Λ is a constant [7]. It comes from the cosmological constant Λ. We also know that the energy of regular matter dilutes as $1/a^3(t)$ when the Universe expands. Therefore, we can express the energy density as

$$\rho = \frac{3H_0^2}{8\pi G}\left(\Omega_\Lambda + \Omega_M\big(\frac{a_0}{a}\big)^3\right) \tag{29}$$

where Ω_M is the normalized energy density of regular matter and Ω_Λ is the energy density of the vacuum. Thus plugging the above equation into Eq. 11, we obtain a differential expression between the radial coordinate r and the time t as

$$dt = \frac{dx}{H_0 x\sqrt{\Omega_\Lambda + \Omega_M x^{-3}}} \tag{30}$$

where $x \equiv a/a_0 = 1/(1+z)$. Next, we use the integral relation defined in Eq. 13, plug dx to replace dt and get an integral form of the light path length d_p. Using the relation between d_p and d_L expressed in Eq. 23, we find an integral form of the luminosity distance as

$$d_L = \frac{1+z}{H_0}\int_0^z \frac{dz'}{\sqrt{\Omega_M(1+z')^3 + \Omega_\Lambda)}}. \tag{31}$$

We can use Eq. 31 to deduce Ω_Λ and Ω_M when we have enough data points for the luminosity distance d_L and the redshift z.

2.4 Acceleration of the Expansion

Now that we can use Eq. 31 to find Ω_Λ and Ω_M, in this section, we will see how the measurements of Ω_M and Ω_Λ are related to the deceleration parameter q_0 [7].

According to the discussion in Weinberg [7], the ratio between the pressure p and the density ρ is zero for regular matter and -1 for vacuum energy. Thus, based on the definition of ρ_c in Eq. 27 and Ω in Eq. 28, we have the total pressure p_0 and total energy ρ_0 as

$$p_0 = \frac{3H_0^2}{8\pi G}(-\Omega_\Lambda) \tag{32a}$$

$$\rho_0 = \frac{3H_0^2}{8\pi G}(\Omega_M + \Omega_\Lambda). \tag{32b}$$

Then from the definition of deceleration parameter q_0 and the Friedmann equation in Eq. 10, we have

$$q_0 \equiv -\frac{\ddot{a}a}{\dot{a}^2} = \frac{1}{2}(\rho_0 + 3p_0). \tag{33}$$

Plugging Eq. 32 into this equation, we have the relation between the deceleration parameter q_0 and the cosmological parameters

$$q_0 = \frac{1}{2}(\Omega_M - 2\Omega_\Lambda). \tag{34}$$

Therefore, when we have values for Ω_M and Ω_Λ, we can calculate the deceleration parameter and decide if the expansion is accelerating or decelerating.

3 Experimental Procedures and Results

3.1 Standard candle

We have seen from Eq. 4 that we need the luminosity L to measure the luminosity distance. Fortunately, there are classes of celestial events in the Universe with predictable luminosities, which are called standard candles [7].

At the beginning of this paper, we have mentioned the variable stars, one class of standard candles discovered by Leavitt. However, they are not bright enough for the task of learning about the expansion of

the Universe: they can only be identified at a distance of 10 Mpc. We need a detection range at least 100 times longer [8]. An alternative type of standard candles, Type Ia supernovae, came into our sight [3, 7, 13, 14].

3.2 Type Ia supernova

Back in 1938, the idea of using Type Ia supernovae as standard candles was pioneered by Walter Baade [3]. Type Ia supernovae are bright enough so that their lights can be detected at high-redshift. The validity of the Type Ia supernovae as the standard candles was studied by a group of astrophysicists, with their results published in 1993 [13]. In this section, we are going to look into their mechanism and explain why they are optimal standard candles in this study.

3.2.1 Overview

In order to fully motivate the following text describing the mechanism of a Type Ia supernova, we will first give an overview of the whole process with qualitative descriptions. A Type Ia supernova starts from a white dwarf, a class of very dense celestial objects having the mass of the Sun but the size of the Earth [15]. They have tremendous inward gravitational pressure. The pressure is so huge that classical gas or radiation pressure cannot hold the star from collapsing [15]; another mechanism called electron degeneracy pressure supports the star from inside. Electron degeneracy pressure is a consequence of the Pauli exclusion principle that no two fermions can share the same quantum state. When the electron degeneracy pressure balances the gravitational pressure, the white dwarf is stable. However, a white dwarf can steal matter from a nearby neighbor with its great gravitational effect. As its mass increases, its gravitational pressure increases. At a mass called the Chandrasekhar limit, roughly 1.44 solar masses, the gravitational pressure will overcome the electron degeneracy pressure, so the white dwarf collapses again. The collapse triggers fusion inside the white dwarf, generating a large amount of energy during the supernova.

3.2.2 Electron degeneracy

Electrons are fermions and thus restricted by the Fermi-Dirac distribution. For a group of electrons with energy E in temperature T, the Fermi-Dirac distribution is expressed as [16]

$$f(E) = \frac{1}{1 + e^{(E-\mu)/k_B T}}, \tag{35}$$

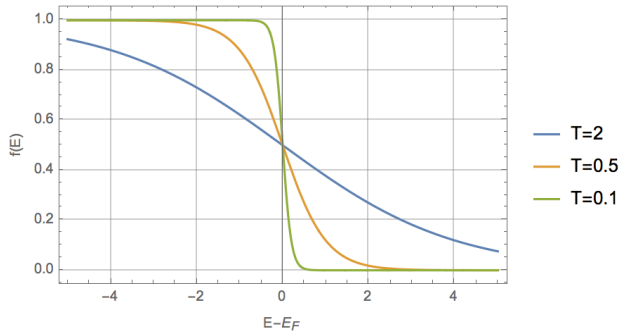

Figure 2: The Fermi-Dirac distribution. In the plot, we set $k_B = 1$ and $\mu = 0$. As temperature T goes to zero, the distribution approximates a stepwise function at μ. We call the energy threshold Fermi energy E_F. In this plot, $E_F = \mu = 0$.

where $f(E)$ is the expected number of electrons with energy E, k_B is the Boltzmann constant and μ is the chemical potential. Since $f(E) < 1$, we can see that two electrons cannot have the same energy. As the temperature T approaches zero, the distribution function becomes a stepwise function with $f(E) = 1$ when $E < \mu$ and $f(E) = 0$ when $E > \mu$. We call the threshold Fermi energy E_F. Fig. 2 shows the distribution as T approaches zero.

Therefore, at low temperature, the electrons go towards energy $E < E_F$. When $T = 0$, all electrons have energy less than the Fermi energy and the system is completely degenerate. When $T > 0$, we do not have complete degeneracy but, under certain conditions, a complete degeneracy can be a good approximation [16].

Next, we are going to derive an expression for the Fermi energy of the electron degeneracy gas. If an electron with mass m_e is inside a box with length l with infinite energy wells around, its energy is [16]

$$E_e = \frac{h^2}{8m_e l^2}(n_x^2 + n_y^2 + n_z^2) \leq \frac{h^2 n_{max}^2}{8m_e l^2} \tag{36}$$

where h is the Planck constant, and n_x, n_y, n_z are principle quantum numbers in all three directions. When the electrons are degenerate, the total energy is limited by the Fermi energy. Thus, the expression $n_x^2+n_y^2+n_z^2$ is capped at some n_{max}^2. If we put all possible values of (n_x, n_y, n_z) in a Cartesian coordinate, we get a 1/8 sphere.

In degenerate electron gas, all the states in the sphere are occupied, so we can relate n_{max} with the total number of electrons N as [16]

$$N = 2 \times \frac{1}{8} \times \frac{4}{3}\pi n_{max}^3. \tag{37}$$

We get the volume of the 1/8-sphere in n-space and multiply it by two since electrons have two spin states. We should also see that n_{max} is a huge number, so it is reasonable to approximate the n-space as continuous. We can rewrite the Eq. 37 equation as

$$n_{max} = \Big(\frac{3N}{\pi}\Big)^{1/3}. \tag{38}$$

Using the 3D infinite square model in Eq. 36 we replace n_{max} with energy E_e, and find the final version of the Fermi energy E_F of the degenerate electron gas to be

$$E_F = \frac{h^2}{8m_e}\Big(\frac{3N}{\pi V}\Big)^{2/3}. \tag{39}$$

We should note that the Fermi energy is the maximum energy a degenerate electron can have. In the above equation, N/V is the number of electrons per volume. We can see that the Fermi energy increases as electrons are more packed together.

3.2.3 White dwarf

Type Ia supernovae start from white dwarfs. Therefore, in this section, we are going to explain what happens inside a white dwarf. We will find that the electrons inside the white dwarf are degenerate, despite the fact that the temperature of the white dwarf core is about 10^7K [15].

When we have a neutral system with density ρ, made up of atoms with Z protons (or electrons) and A nucleons, this system has N/V electrons per volume, Z/A electrons per nucleon and ρ/m_n nucleons per volume. Thus, we can rewrite N/V as

$$\frac{N}{V} = \frac{Z}{A}\frac{\rho}{m_n}, \tag{40}$$

where m_n is the mass of a nucleon. We rewrite the Fermi energy in Eq. 39 as

$$E_F = \frac{h^2}{8m_e}\Big(\frac{3Z\rho}{\pi A m_n}\Big)^{2/3}. \tag{41}$$

We also know that the average kinetic energy of the electron gas is $(3/2)kT$. When the average kinetic energy is below the Fermi energy, we can expect most of the electrons to be degenerate. If the kinetic energy is far less than the Fermi energy, a complete degeneracy would be a good approximation. Thus, for the electrons to be degenerate, we have [15]

$$\frac{T}{\rho^{2/3}} < 1261 \text{ K} \cdot \text{m}^2 \cdot \text{kg}^{-2/3}. \tag{42}$$

When we plug in parameters of a white dwarf, we get values far less than 1261 $\mathrm{K} \cdot \mathrm{m}^2 \cdot \mathrm{kg}^{-2/3}$. For example, for Sirius-B, a white dwarf with about solar mass and Earth size, we get 37 $\mathrm{K} \cdot \mathrm{m}^2 \cdot \mathrm{kg}^{-2/3}$, which is far less than our upper limit [15]. Therefore, although the temperature inside the white dwarf is not close to zero, its overwhelming density raises the Fermi energy enough so that electron gas in a white dwarf is close to a complete degeneracy.

Besides the electron degeneracy, the nuclei in a white dwarf are mostly carbon and oxygen. Because of the high temperature and high density in the white dwarf, small nuclei such as hydrogen or helium will fuse into larger nuclei. Besides, based on observations of the white dwarf luminosities, they would be much brighter if there were fusions inside. Therefore, white dwarfs are mostly made up of carbon and oxygen, since smaller atoms are not stable inside the white dwarf [15].

3.2.4 Electron degeneracy pressure

Degenerate electrons creates an outward pressure that supports the white dwarf from the gravitational pressure. Now that we understand the electrons inside the white dwarf are degenerate, we can calculate its total energy and the electron degeneracy pressure. We have seen from Eq. 38 that n_{max} is large enough to be approximated as continuous. Thus, to calculate the total energy of the degenerate electrons, we integrate the energy of all the electrons inside the 1/8-sphere in n-space of Eq. 36 such that the total energy U is [16]

$$U = 2 \int \int \int_V \frac{h^2}{8m_e l^2}(n_x^2 + n_y^2 + n_z^2) dn_x dn_y dn_z. \tag{43}$$

We multiply by two for electron spin. However, since the n-space is an 1/8-sphere, it is easier to integrate using spherical coordinates.

$$U = 2 \int_0^{n_{max}} n^2 \frac{h^2}{8m_e l^2} n^2 dn \int_0^{\pi/2} \sin\theta d\theta \int_0^{\pi/2} d\phi. \tag{44}$$

We calculate the integral with the relation between n_{max} and N expressed in Eq. 38 and the energy limit in Eq. 36. We find the energy of the degenerate electron gas to be

$$U = \frac{3}{5} N E_F. \tag{45}$$

Then, using $P = dU/dV$ and the Fermi energy in Eq. 39, we get the electron degeneracy pressure as

$$P_e = \frac{h^2}{20m_e}\Big(\frac{3}{\pi}\Big)^{2/3} n_e^{5/3} \tag{46}$$

where $n_e \equiv N/V$ is the number of electrons per unit volume.

3.2.5 Chandrasekhar limit and the supernova

The Chandrasekhar limit is the mass limit where the mass of the white dwarf is so large that the electron degeneracy pressure can no longer balance the gravitational pressure. From Newtonian mechanics, we obtain the gravitational potential energy of the white dwarf as [16]

$$U_g = -\frac{3}{5}GM^2\Big(\frac{4\pi}{3V}\Big)^{1/4} \tag{47}$$

where G is the gravitational constant and M is the mass of the white dwarf. Using $P = dU/dV$, we have [16]

$$P_g = \frac{G}{5}\Big(\frac{4\pi}{3}\Big)^{1/3} M^{2/3}(2m_n)^{4/3} n_e^{4/3}. \tag{48}$$

The critical mass is the mass when the gravitational pressure balances the electron degeneracy pressure expressed in Eq. 46. Equaling the two expressions, we find the critical mass to be

$$M = \Big(\frac{3h^2}{4\pi m_e G}\Big)^{3/2} \frac{n_e^{1/2}}{8m_n^2}. \tag{49}$$

We know that the electron degeneracy pressure can hold the gravitational pressure only if the electrons inside are non-relativistic [16]. Using the non-relativistic condition $p_e < m_e c$ where $p_e = \sqrt{2m_e E_F}$ is the upper limit of the momentum of the electron, we find the limit for the electron density n_e to be

$$n_e < \frac{8\pi}{3}\Big(\frac{m_e c}{h}\Big)^3. \tag{50}$$

Thus the constraint on n_e limits the critical mass in Eq. 49 to be $M < 2.462 \times 10^{30}$ kg=$1.24M_\odot$. In our derivation, we assume that the density of the white dwarf is a constant. However, if we use a more realistic density distribution that changes radially, we find that $M < 1.44M_\odot$, which is the Chandrasekhar limit [15]. We have not found a white dwarf with a mass greater than the Chandrasekhar limit [15].

Therefore, when the mass of the white dwarf goes over the Chandrasekhar limit, it collapses and the

temperature inside the white dwarf increases drastically. The carbon and oxygen in the white dwarf undergo a series of uncontrolled nuclear fusions, producing a variety of nuclei ranging from sodium to nickel, including silicon. Thus, Type Ia supernovae show Si II absorption lines. It is also important to note here that Type Ia supernovae do not have hydrogen lines because white dwarfs do not contain hydrogen. Although the fusions produce a wide range of nuclei besides silicon, we use Si II lines to identify Type Ia supernovae from other Type I supernovae. The fusions release a great amount of energy and destroy the white dwarf into a supernovae remnant [15][6]. We can see these spectral characteristics from the three example spectra shown in Fig. 3.

3.2.6 Type Ia supernovae as standard candles

Type Ia supernovae are optimal to serve as the standard candles because they are very bright and easy to identify. Because of the Chandrasekhar limit, the initial amount of fuel for the fusion is relatively uniform. Thus, most of the Type Ia supernovae have an absolute magnitude of -19.3 ± 0.3 [15][7].

Type Ia supernovae are also very bright. They are about 10^{10} times more luminous than the Sun. In fact, they are the most luminous of all types of supernovae [15]. They can be seen from several thousand megaparsecs [7]. Thus, it is easier to observe them from a long distance, which is pivotal to the success of this experiment.

In addition, we can easily identify a Type Ia supernova from its spectral structure. All types of Type I supernovae do not have hydrogen absorption lines since small atoms like hydrogen are not stable inside a white dwarf. The absence of hydrogen absorption lines makes the spectra very uncommon because hydrogen is the most abundant element in the Universe. Besides, they often have Si II absorption lines since the carbon-oxygen fusion process creates silicon nuclei [8, 15]. We can see these features in the example spectra in Fig. 3 [15].

Therefore, Type Ia supernovae are very bright. They are bright enough to make observations at high redshift. Their spectra are also uncommon, with the absence of hydrogen lines and the existence of Si II line. We can confirm the detection of Type Ia supernova easily. Those properties make Type Ia supernovae excellent standard candles for higher redshift measurements.

[6]The exact mechanism of Type Ia supernovae remains unknown to us. Physicists have built different models but none of them has been confirmed yet [17].

[7]Absolute magnitude is a quantity used since ancient astronomy to indicate luminosity. The lower it is, the brighter the source. The Sun has an absolute magnitude of +4.77 [15]. A difference of five in magnitude is 100 times in luminosity. Thus, a typical Type Ia supernova is about 10^{10} times more luminous than the Sun

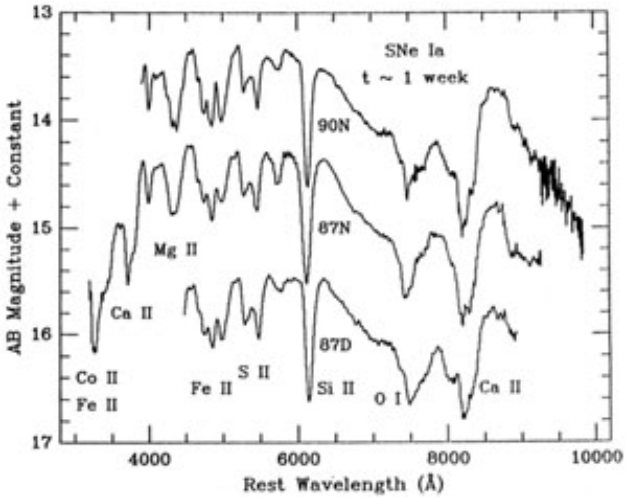

Figure 3: Three example spectra of Type Ia supernovae (SN 1987D, SN 1987N, and SN 1990N), measured one week after peak luminosity [18]. We can see the absence of hydrogen lines and the strong existence of the Si II line.

3.3 Charge-coupled device (CCD)

The idea of using Type Ia supernovae as standard candles to measure the acceleration of the expansion had existed for a long time before the Nobel Laureates started the projects in the 1990s [3]. Unlike the variable stars, the supernovae only last for weeks [7]. We did not have a systematic way to detect them. Another difficulty is that the light becomes too dim at high redshift, so it is hard for traditional devices to make reasonable observations of the brightness. The invention of CCDs solves all these problems.

The usage of CCD revolutionized observational astronomy studies [20]. Because of its low noise, it is much more sensitive to light at a low intensity. Therefore, they are very useful in the detection of high-redshift supernovae.

As is shown in Fig. 4a, a CCD has a two-dimensional array of photoelectronic chips, which is called the active area [20]. Each chip represents a pixel in the image. We want to expose the CCD to light and see how many photons each pixel receives during the exposure to create the image. In a more complicated CCD, prisms are used to separate the light into different colors [20].

CCDs detect light with the photoelectric effect. A photon with sufficient energy, usually 1.1 to 4eV [20], hits the active area and frees an electron. Then the electron will fall into an artificial energy well. Figure 4b shows a three-phase pixel, with three steps 0V, 5V and 10V. When a photon hits the device, the electron created always lands into the 0V well.

After the exposure duration ends, the pixel wells collect enough electrons [20]. Fig. 4b shows how we

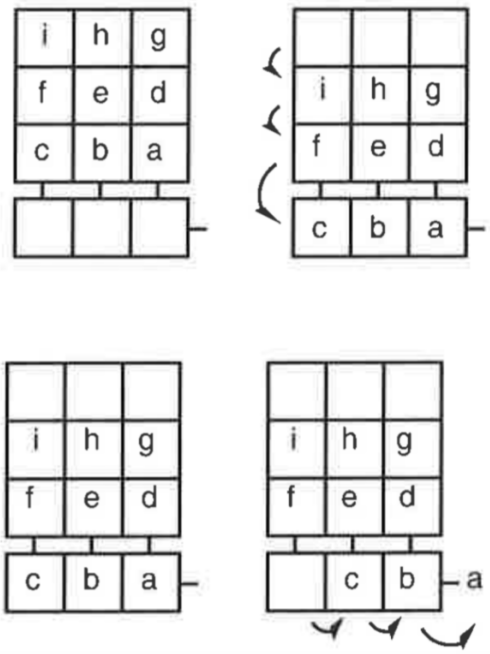

(a) The shifting of a CCD on the macroscopic scale [19]. We move one row into the output row. Then, we shift the whole output row out to the right and collect the intensities at each pixel. We keep shifting the rows until we have the intensities at all the pixels.

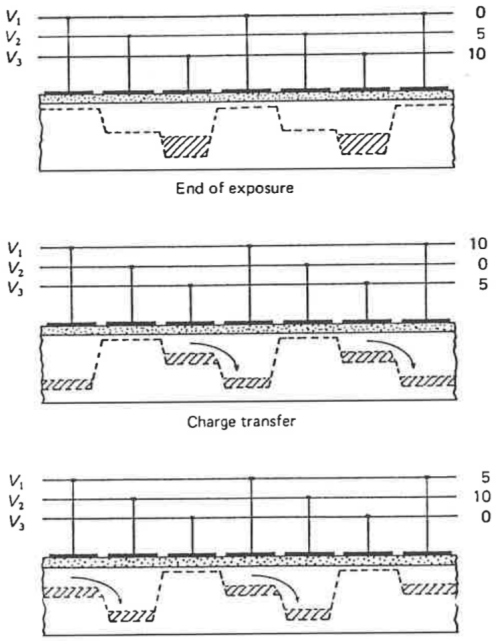

(b) The shifting of a three-phase CCD on the pixel scale [20]. Initially, the electrons are in the 0V bucket. When we rotate the energy levels, the 0V electrons are raised up to 5V. The electrons tend to stay in the lowest energy well, so they will move to the right into the next bucket. Therefore, by manipulating the energy wells, we can move the electrons around on the CCD.

Figure 4: Mechanism of a CCD.

manipulate the energy wells to move them around. We rotate the energy steps, changing 0V to 5V, 5V to 10V and 10V back to 0V. Since the electrons always go to the 0V well, they will move in the direction of our rotations.

The rotation happens every clock tick. For a three-phase CCD, after three clock ticks, the electrons at the end of the rows will move out of the active area, where they enter an additional row of pixels. Then we shift the extra row horizontally in the same way to the output at the corner of the device, where a computer collects the intensities at each pixel. Figure 4a shows this process. We keep shifting the rows and columns until we get the intensities at all pixels.

We store the intensity in every pixel in a computer, which means that we can restore the picture afterwards. Therefore, if we can take pictures periodically and compare the sky at the same location at different times with the image processing technology, we can systematically search for high-redshift supernovae in the sky [5].

Therefore, the invention of CCDs is pivotal in measuring the acceleration of the Universe expansion. The CCDs give us a systematic way to search for Type Ia supernovae in the sky so that we can collect enough data. In addition, they also enable us to observe high-redshift supernovae due to their high sensitivity to photons.

3.4 Experiment results

With the help of CCDs, astronomers started the projects of searching for Type Ia supernovae at the end of the last century and published their results on the expansion of the Universe in the late 1990s [4, 5, 21].

The astronomers observed a total of 42 Type Ia supernovae and published the results in 1998 [4, 5]. With these data, it became possible to measure Ω_M and Ω_Λ and calculate the deceleration parameter.

3.4.1 Measurements of Ω_M and Ω_Λ

We present the experimental results in Fig. 5. The quantity on the y-axis in Fig. 5 is the bolometric magnitude m_B, where the term "bolometric" means the magnitude considers the whole spectrum. The relation between the bolometric magnitude m_B and the luminosity distance d_L is

$$m_B = 5log_{10}(d_L) + C \tag{51}$$

where C is a constant[8]. From Fig. 5, we can see that higher redshift is correlated to a higher magnitude. A higher redshift means a longer distance by Hubble's law, and higher magnitude means lower brightness by Eq. 51. The relation in Fig. 5 makes sense: the further the source is, the dimmer it would be.

We plot the predictions of several models in Fig. 5. The blue ones are predictions assuming a flat Universe. By statistically fitting Eq. 31 into the data, we find that the best fit gives $\Omega_\Lambda = 0.72$ and $\Omega_M = 0.28$ for a flat Universe [5]. This means that under a flat Universe assumption, which is close to the truth on a cosmological scale [12], the vacuum energy takes up about 72% of the Universe while regular matter takes only about 28%. Therefore, vacuum energy dominates the Universe, the nature of which still remains as one of the most intriguing mysteries in modern physics.

[8]For a full description of the relation between luminosity distance and m_B, please refer to [7]. To proceed on with this discussion, it is sufficient to understand that m_B is proportional to $log_{10}(d_L)$.

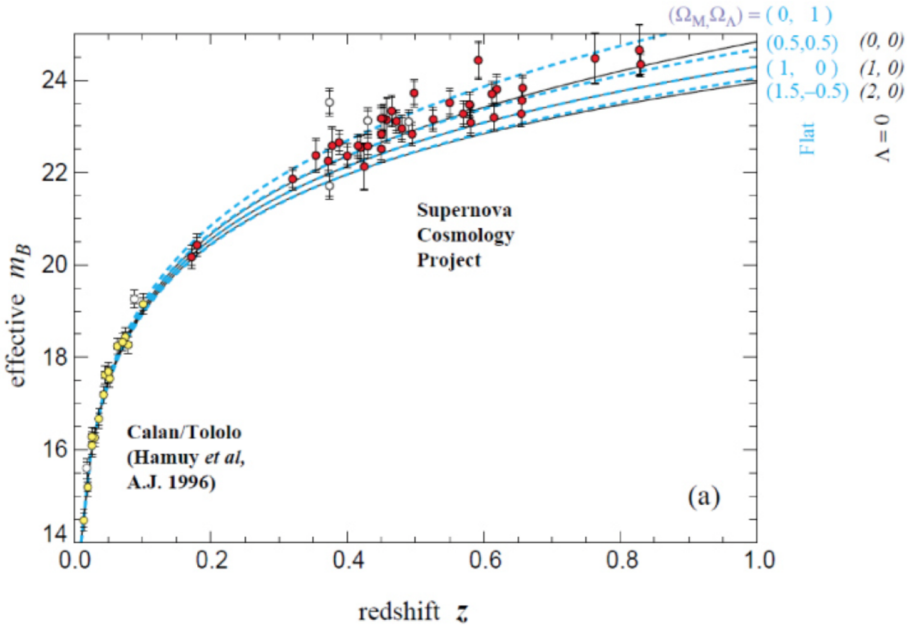

Figure 5: Plot of 60 Type Ia supernovae with the redshift on the x-axis and magnitude on the y-axis, with curves predicted by some typical model [5]. The optimal fit for this data is $\Omega_\Lambda = 0.72$ and $\Omega_M = 0.28$ if we assume a flat Universe.

3.4.2 Acceleration of the Expansion

Based on the data in Fig. 5, we construct confidence domains of Ω_Λ and Ω_M in Fig. 6. Figure 6 shows the 68% confidence region and 90% confidence region in blue shade. The dashed line is for $\ddot{q} = 0$ in Eq. 33 where the Universe expansion is neither accelerating nor decelerating. Using the best fit values of $\Omega_\Lambda = 0.72$ and $\Omega_M = 0.28$, we find the deceleration parameter to be -0.58. A negative q_0 indicates an accelerating expansion. Also, from Fig. 6, we can see that the 90% confidence contour is above the dashed line. Therefore, based on the experimental data, we can conclude that, with at least 90% confidence, the expansion of the Universe is accelerating.

4 Conclusion

In this paper, we take a comprehensive investigation into the expansion of the Universe. Following the steps of the Nobel Laureates of 2011, we look at both the theoretical side and the experimental side of this study.

The center of the theoretical part of this study is the relation between the luminosity distance and redshift. We can directly calculate both of them from observations of Type Ia supernovae. We set up

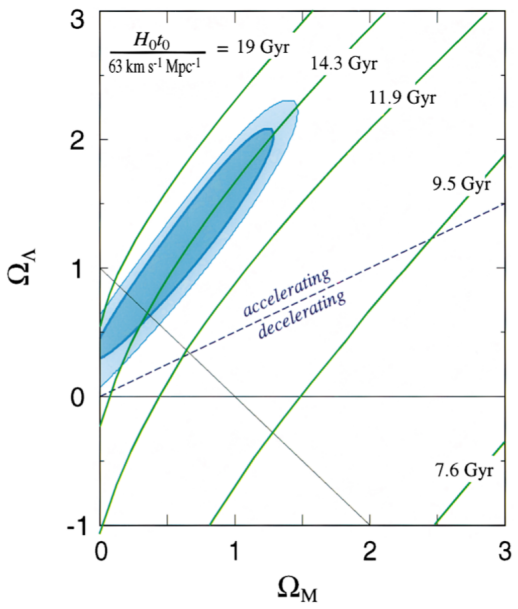

Figure 6: Estimations of Ω_Λ and Ω_M [5]. The plot shows the 68% and 90% confidence domains as blue-shaded areas. The dashed line is the stable line where the expansion is neither decelerating nor accelerating, given as $q_0 = 0$ in Eq. 33.

the fundamentals by defining the redshift and luminosity distance in the context of the Robertson-Walker metric. We plug the metric into the Einstein equation which leads us to the Friedmann equations. Based on this infrastructure, we derive the relation between luminosity distance and redshift in a series form and an integral form. The series form of the relation tells us that we need to make measurements at higher redshifts to see the effects of the acceleration. Then, assuming the Universe consists of regular energy and vacuum energy, we derive the integral form of the luminosity distance-redshift relation. We use the integral form to find the energy components. Finally, we derive an explicit relation between the deceleration parameter and the energy density components.

Moving into the experimental part, we talk about the concept of standard candles, which are celestial events with known luminosities. Variable stars are the first standard candles discovered, but they are too dim at high redshift. Baade proposed that we could use Type Ia supernovae as standard candles [3]. They are very bright and easy to identify. However, Type Ia supernovae are rare and only last for weeks. At that time, we did not have the technology to detect them systematically at high redshift. By the end of the 20th century, with the advance of CCD and information technologies, we were able to detect a significant number of Type Ia supernovae and measure the acceleration of the expansion.

Based on the data collected, we find that the Universe expansion is accelerating. Vacuum energy, which

dominates about 3/4 of the Universe, drives the expansion. We plot the confidence domain and conclude with at least 90% confidence that the expansion of the Universe is accelerating.

This study raises more questions than it solves. We find the Universe expansion is accelerating. However, we attribute the acceleration to a quantity we know almost nothing about, the vacuum energy. Especially, we claim that the vacuum energy dominates about three-quarters of the Universe. Since then, physicists have put a lot of effort to understand the vacuum energy. One of the most successful theories is the Standard Model, coming from particle physics. The Standard Model proposes two sources of the vacuum energy: quantum fluctuations and spontaneous symmetry breaking. However, its prediction of vacuum energy is 10^{122} times greater than the measurements. There are other efforts towards an understanding of the vacuum energy as well; however, for the time being, the nature of vacuum energy is still a mystery [8].

5 Acknowledgement

This research is supported by Carleton College. We thank our professors from Carleton College who provided insights and expertise that greatly facilitated the research process. Particularly, we thank Professor Frank McNally for advising this study, and Professor Jay Tasson for offering help in cosmology and general relativity.

References

[1] Nobelprize.org. *The Nobel Prize in Physics 2011 - Advanced Information.* URL: `https://www.nobelprize.org/nobel_prizes/physics/laureates/2011/popular.html` (visited on 02/05/2018).

[2] Vesto Melvin Slipher. "The radial velocity of the Andromeda Nebula". In: *Lowell Observatory Bulletin* 2 (1913). redshift pioneer, pp. 56–57.

[3] Walter Baade. "The Absolute Photographic Magnitude of Supernovae." In: *The Astrophysical Journal* 88 (1938). supernova pioneer, p. 285.

[4] Adam G Riess et al. "Observational evidence from supernovae for an accelerating universe and a cosmological constant". In: *The Astronomical Journal* 116.3 (1998). breakthrough 1. History. Expression of luminosity distance. mb vs. omegas, p. 1009.

[5] Saul Perlmutter et al. "Measurements of Ω and Λ from 42 high-redshift supernovae". In: *The Astrophysical Journal* 517.2 (1999). breakthrough 2, p. 565.

[6] Edwin Hubble. "A relation between distance and radial velocity among extra-galactic nebulae". In: *Proceedings of the National Academy of Sciences* 15.3 (1929), pp. 168–173.

[7] Steven Weinberg. *Cosmology*. 43 luminosity distance, 106 flat universe, 46 validility of using supernova, 27 supernova mechanism, 18 magnetude-lumi relation. Oxford University Press, 2008.

[8] Nobelprize.org. *The Nobel Prize in Physics 2011 - Advanced Information*. URL: `https://www.nobelprize.org/nobel_prizes/physics/laureates/2011/advanced.html` (visited on 02/05/2018).

[9] William C Keel. *The road to galaxy formation*. cosmo principle. Springer Science & Business Media, 2007.

[10] James Schombert. *Cosmological Principle*. 2015. URL: `http://abyss.uoregon.edu/~js/cosmo/lectures/lec05.html` (visited on 03/25/2018).

[11] Thomas Andrew Moore. *A General Relativity Workbook*. University Science Books Mill Valley, 2013.

[12] Pea de Bernardis et al. "A flat Universe from high-resolution maps of the cosmic microwave background radiation". In: *Nature* 404.6781 (2000). Justifying the flat universe assumption, p. 955.

[13] Mario Hamuy et al. "The 1990 calan/tololo supernova search". In: *The Astronomical Journal* 106 (1993). usefulness of supernova, low z detection, pp. 2392–2407.

[14] CT Kowal. "Absolute magnitudes of supernovae." In: *The Astronomical Journal* 73 (1968), pp. 1021–1024.

[15] Bradley W Carroll and Dale A Ostlie. *An introduction to modern astrophysics*. Cambridge University Press, 2017.

[16] Stefan Westerhoff. *Thermal Physics Course Notes to Schroeder*. (unpublished). 2015.

[17] David Branch. *TYPE Ia SUPERNOVAE AS STANDARD CANDLES*. 1992. URL: `https://ned.ipac.caltech.edu/level5/Branch2/Branch_contents.html` (visited on 03/26/2018).

[18] AV Filippenko. "SN 1987A and Other Supernovae, ed". In: *IJ Danziger & K. Kjär (ESO: Garching)* 343 (1991).

[19] Patrick Martinez and Alain Klotz. *A practical guide to CCD astronomy*. Vol. 8. Cambridge University Press, 1998.

[20] Steve B Howell. *Handbook of CCD astronomy*. Vol. 5. Cambridge University Press, 2006.

[21] Saul Perlmutter et al. “Measurements* of the Cosmological Parameters Ω and Λ from the First Seven Supernovae at z≥ 0.35”. In: *The astrophysical journal* 483.2 (1997). P97 referred to in breakthrough paper, contains more details about the method., p. 565.